Cardiovascular Research Advance Access published August 24, 2008

Cardiovascular Research
doi:10.1093/cvr/cvn205

Nitric oxide inhibits Kv4.3 and human cardiac transient outward potassium current (I_{to1})

Ricardo Gómez[1†], Lucía Núñez[1†], Miguel Vaquero[1], Irene Amorós[1], Adriana Barana[1], Teresa de Prada[2], Carlos Macaya[2], Luis Maroto[3], Enrique Rodríguez[3], Ricardo Caballero[1]*, Antonio López-Farré[2], Juan Tamargo[1], and Eva Delpón[1]

[1]*Department of Pharmacology, School of Medicine, Universidad Complutense, 28040 Madrid, Spain;* [2]*Cardiovascular Research Unit, Hospital Clínico San Carlos, Madrid, Spain; and* [3]*Cardiac Surgery Department, Hospital Clínico San Carlos, Madrid, Spain*

Received 3 March 2008; revised 18 July 2008; accepted 24 July 2008

Time for primary review: 27 days

KEYWORDS
Atrial fibrillation;
Nitric oxide;
Human transient outward current;
Patch clamp;
Kv4.3 channels

Aims Chronic atrial fibrillation (CAF) is characterized by a shortening of the plateau phase of the action potentials (AP) and a decrease in the bioavailability of nitric oxide (NO). In this study, we analysed the effects of NO on Kv4.3 ($I_{Kv4.3}$) and on human transient outward K^+ (I_{to1}) currents as well as the signalling pathways responsible for them. We also analysed the expression of NO synthase 3 (NOS3) in patients with CAF.

Methods and results $I_{Kv4.3}$ and I_{to1} currents were recorded in Chinese hamster ovary cells and in human atrial and mouse ventricular dissociated myocytes using the whole-cell patch clamp. The expression of NOS3 was analysed by western blotting. AP were recorded using conventional microelectrode techniques in mouse atrial preparations. NO and NO donors inhibited $I_{Kv4.3}$ and human I_{to1} in a concentration- and voltage-dependent manner (IC_{50} for NO: 375.0 ± 48 nM) as a consequence of the activation of adenylate cyclase and the subsequent activation of the cAMP-dependent protein kinase and the serine–threonine phosphatase 2A. The density of the I_{to1} recorded in ventricular myocytes from wild-type (WT) and NOS3-deficient mice ($NOS3^{-/-}$) was not significantly different. Furthermore, the duration of atrial AP repolarization in WT and $NOS3^{-/-}$ mice was not different. The increase in NO levels to 200 nM prolonged the plateau phase of the mouse atrial AP and lengthened the AP duration measured at 20 and 50% of repolarization of the human atrial CAF-remodelled AP as determined using a mathematical model. However, the expression of NOS3 was not modified in left atrial appendages from CAF patients.

Conclusion Our results suggested that the increase in the atrial NO bioavailability could partially restore the duration of the plateau phase of CAF-remodelled AP by inhibiting the I_{to1} as a result of the activation of non-canonical enzymatic pathways.

1. Introduction

Atrial fibrillation (AF), the most common sustained cardiac arrhythmia, alters atrial electrophysiology in a way that promotes its occurrence and persistence, a phenomenon called 'electrical remodelling', which is mainly characterized by a marked shortening of the plateau and the final phase of repolarization of human atrial action potential (AP).[1]

Nitric oxide (NO), a diffusible messenger produced by all myocardial cell types, has important effects on cardiac function including rate, contraction, relaxation, coronary reserve, platelet aggregation, mitochondrial respiration, cell growth, and survival.[2] In a porcine model, AF induced an 'endocardial dysfunction', characterized by a marked decrease in NO synthase 3 (NOS3) expression and the corresponding drop in NO concentration.[3] Currently, it is unknown whether human chronic AF (CAF) also decreases NOS3 atrial expression, but it is clearly established, both in patients and in animal models, that NO bioavailability decreases in AF because of an increased atrial oxidative stress.[4,5]

The height and the duration of the plateau phase of the human atrial AP are determined by the balance between the inward L-type Ca^{2+} current (I_{CaL}) and several outward K^+ currents.[6] The effects of NO on I_{CaL} have been studied in cardiac myocytes from different species and in cloned channels expressed in heterologous systems.[7,8] Previous reports demonstrated that NO inhibits the rapid component of the delayed rectifier current (I_{Kr}),[9] whereas it increases the slow component (I_{Ks}).[10] More recently, we have described that NO blocks hKv1.5 channels, which generate the ultrarapid delayed rectifier K^+ current (I_{Kur}).[11]

* Corresponding author. Tel: +34 34913941474; fax: +34 913941470.
E-mail address: rcaballero@med.ucm.es
† These two authors contributed equally.

However, the effects of NO on the Ca^{2+}-independent component of the transient outward K^+ current (I_{to1}) are presently unknown. Human cardiac I_{to1} is predominantly carried by Kv4.3 α-subunits, which assemble with KChIPs, DPP6, and probably also MiRPs ancillary subunits.[12] Thus, this study aimed to analyse the effects of NO on Kv4.3 current ($I_{Kv4.3}$) and on human atrial I_{to1}, as well as the intracellular signalling pathway responsible for the effects. Our results suggested that the increase in atrial NO bioavailability could partially restore the duration of the plateau phase of CAF-remodelled AP by inhibiting the I_{to1} as a result of the activation of non-canonical enzymatic pathways.

2. Methods

The study was approved by the Ethics Committee of the Hospital Clínico San Carlos de Madrid (No. B-05/017) and conforms with the principles outlined in the Declaration of Helsinki. Each patient gave written informed consent.

2.1 Western blotting of human atrial appendages

NOS3 expression was determined in left atrial appendages (LAA) from sinus rhythm (SR) or CAF patients by western blot analysis as described.[3] Patient characteristics are shown in *Table 1*. To determine S-nitrosylated Kv4.3 channels, the biotin-switch assay followed by western blot was performed.[11]

2.2 Cell culture, human and mouse myocyte isolation, and solutions

Chinese hamster ovary (CHO) cells were transiently transfected with the cDNA encoding Kv4.3 as described previously.[13,14] Cells were perfused with an external solution containing (mM): NaCl 136, KCl 4, $CaCl_2$ 1.8, $MgCl_2$ 1, HEPES 10, and glucose 10 (pH 7.4 with NaOH). Human atrial myocytes were isolated from LAA obtained from patients in SR undergoing cardiac surgery as described.[15] For each group of experiments, myocytes were obtained from at least four patients. Mouse ventricular myocytes were enzymatically isolated[11,13,14] from wild-type (WT) (C57BL/6J strain) and NOS3-deficient ($NOS3^{-/-}$) 12-week-old mice (The Jackson Laboratory). The investigation conforms with the *Guide for the Care and Use of Laboratory Animals* (NIH Publication No. 85-23, revised 1996). For measurements of human and mouse I_{to1}, 2 mM $CoCl_2$ was added to the external solution for blocking I_{CaL}. Recording pipettes were filled with internal solution containing (mM): K-aspartate 80, KCl 42, KH_2PO_4 10, MgATP 5, phosphocreatine 3, HEPES 5, and EGTA 5 (pH 7.2 with KOH). The NO donors ($\pm$)-*S*-nitroso-*N*-acetylpenicillamine (SNAP, Calbiochem) and 2-(*N*, *N*-diethylamine)-diazenolate-2-oxide (DEANO, Sigma) were initially dissolved in ethanol and water, respectively, to yield 10 mM stock solutions. NO donor solutions were freshly prepared for each experiment, and the NO-saturated solution was prepared as described previously.[11] NO concentration in the perfusing chamber was measured using a potentiometric NO sensor.

Table 1 Patient characteristics

	SR ($n = 10$)	CAF ($n = 7$)
Gender	1F/9M	5F/2M
Age (years)	71.6 $\pm$ 2.3	66.7 $\pm$ 2.0
Diabetes (*n*)	6	2
Hyperlipidaemia (*n*)	6	2
Hypertension (*n*)	8	3
Left atrial diameter (mm)	41.8 $\pm$ 3.4	63.1 $\pm$ 2.9*
Lipid-lowering drugs (*n*)	6	3
ACE-I + ARB (*n*)	3	3
β-Blockers (*n*)	6	2

ACE-I, angiotensin-converting enzyme-inhibitors; ARB, angiotensin II receptor blockers; F, female; M, male.
*$P < 0.01$ vs. SR.

2.3 Recording techniques

$I_{Kv4.3}$ and I_{to1} were recorded using the whole-cell patch clamp technique at 21–23°C with Axopatch-200B amplifiers (Molecular Devices). Capacitance and series resistance were optimized and ~80% compensation was usually obtained. In CHO cells, mean maximum $I_{Kv4.3}$ amplitude, uncompensated access resistance (R_a), and cell capacitance (C_m) were 2.5 $\pm$ 0.4 nA, 1.7 $\pm$ 0.2 MΩ, and 14.8 $\pm$ 0.7 pF, respectively ($n = 37$). In human atrial myocytes, the maximum outward K^+ current amplitude averaged 798.5 $\pm$ 126.9 pA, whereas the mean values of C_m and R_a were 115.3 $\pm$ 16.2 pF and 2.0 $\pm$ 0.3 MΩ, respectively ($n = 21$). There were no differences in the C_m from WT and $NOS3^{-/-}$ myocytes (126 $\pm$ 17 pF). In these cells, maximum outward current and R_a were 2.3 $\pm$ 0.3 nA and 1.6 $\pm$ 0.1 MΩ, respectively ($n = 12$). Thus, under our experimental conditions, no significant voltage errors (<5 mV) due to series resistance were expected with the micropipettes used (tip resistance < 3.5 MΩ).

AP were recorded at 34°C in mouse left atria superfused with Tyrode solution (mM: NaCl 137, KCl 5.4, $MgCl_2$ 1.0, $CaCl_2$ 1.8, NaH_2PO_4 0.42, $NaHCO_3$ 11, and glucose 10), bubbled with 95% O_2/5% CO_2, and driven at 3 Hz using conventional microelectrode techniques.[14]

2.4 Mathematical modelling of a human atrial action potential

For simulating the shapes of human atrial AP under non-AF- and AF-modified conditions, we employed a mathematical model. To simulate the electrophysiological remodelling in CAF, reductions of 70% in I_{CaL}, and of 50% in I_{to1} and I_{Kur}, were introduced as described.[16] The model was run at a frequency of 1 Hz in the absence and presence of 200 nM NO by incorporating the specific conductance and time- and voltage-dependent modifications induced by NO on I_{to1}, I_{Kur}, I_{Kr}, I_{Ks}, I_{CaL}, and I_{Na}.

2.5 Statistical methods

Results are expressed as mean $\pm$ SEM. Data were compared by ANOVA followed by the Newman–Keuls test. A value of $P < 0.05$ was considered significant.

3. Results

3.1 Effects of nitric oxide and nitric oxide donors on $I_{Kv4.3}$

Figure 1A shows $I_{Kv4.3}$ traces recorded by applying 250 ms pulses from -80 to $+50$ mV under control conditions and in the presence of 200 μM SNAP. The NO donor reduced the peak $I_{Kv4.3}$ by 30.8 $\pm$ 4.5% ($n = 7$) without modifying the time course of inactivation measured from the bi-exponential fit to the current traces (*Table 2*). SNAP reduced the K^+ efflux crossing the membrane through Kv4.3 channels (charge), estimated from current–time integrals at +50 mV, by 37.5 $\pm$ 1.3%, a reduction not significantly different from that measured at the peak ($P > 0.05$). For this reason, the reduction of the peak current amplitude was used as an index of steady-state inhibition. *Figure 1B* shows the time course of NO release during the development

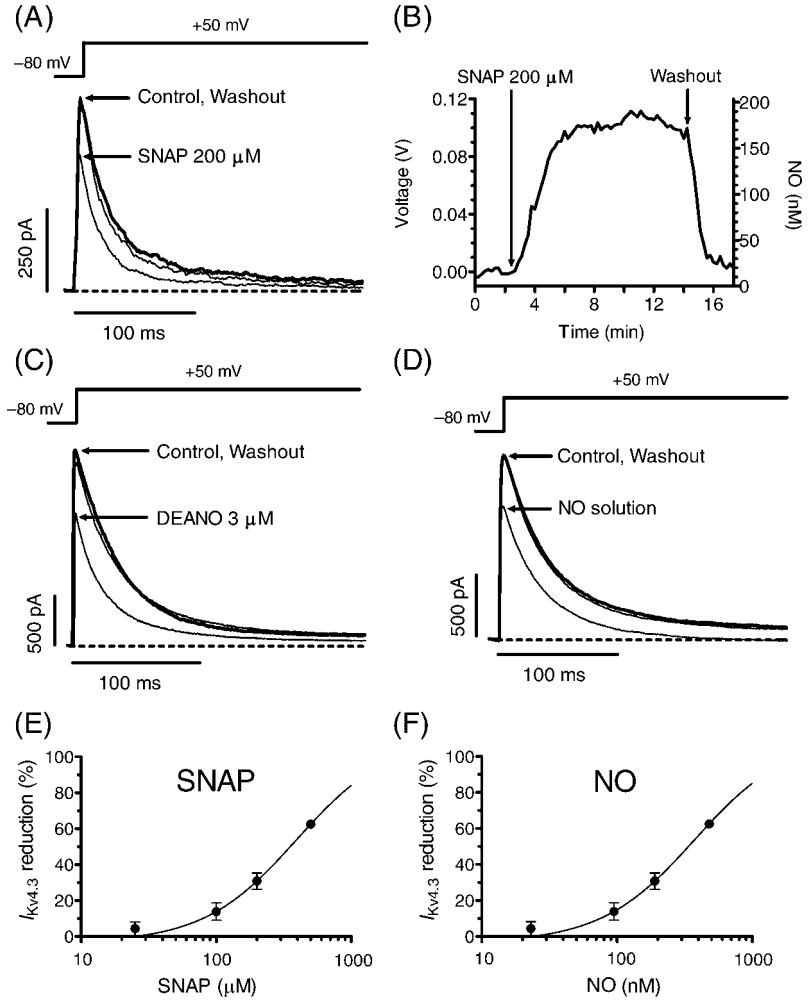

Figure 1 $I_{Kv4.3}$ recorded in Chinese hamster ovary cells in the absence, presence, and after washout of *S*-nitroso-*N*-acetylpenicillamine (SNAP) (*A*), 2-(*N*, *N*-diethylamine)-diazenolate-2-oxide (DEANO) (*C*), and nitric oxide (NO)-saturated solution (*D*). (B) Nitric oxide concentrations yielded before and after the perfusion of *S*-nitroso-*N*-acetylpenicillamine measured using a potentiometric nitric oxide sensor. Percentage of $I_{Kv4.3}$ reduction induced by *S*-nitroso-*N*-acetylpenicillamine as a function of *S*-nitroso-*N*-acetylpenicillamine concentrations (*E*) and the released nitric oxide (*F*). Continuous lines represent the Hill equation fit to the data. Each point represents the mean ± SEM of five or more experiments.

Table 2 Effects of nitric oxide and nitric oxide donors on $I_{Kv4.3}$

	$\tau_{f\ inactivation}$ (ms)		$\tau_{s\ inactivation}$ (ms)		$V_{h\ inactivation}$ (mV)		$k_{inactivation}$ (mV)	
	Control	Drug	Control	Drug	Control	Drug	Control	Drug
SNAP	25.2 ± 4.3	21.7 ± 3.6	114.9 ± 27.5	129.2 ± 27.9	−31.9 ± 3.0	−39.7 ± 3.1*	5.5 ± 0.2	5.9 ± 0.4
NO	35.7 ± 8.5	29.9 ± 4.3	117.7 ± 28.6	98.6 ± 10.5	−32.6 ± 0.4	−40.4 ± 1.1*	5.6 ± 0.2	5.3 ± 0.1
DEANO	30.7 ± 7.1	30.2 ± 5.7	102.6 ± 25.7	107.6 ± 23.5	−30.8 ± 2.4	−42.7 ± 1.3*	4.7 ± 0.2	4.2 ± 0.3

τ, time constant; V_h and k, midpoint and slope of the inactivation curve. Data represent the mean ± SEM of six or more experiments.
*$P < 0.01$ vs. control.

of the experiment (*Figure 1A*). NO concentration reached a maximum within 3–4 min (192 ± 15 nM, $n = 7$) and remained stable during SNAP perfusion (8–10 min), decreasing to basal levels after perfusion with SNAP-free solution.

The effects of another NO donor, DEANO (3 μM), and an NO-saturated solution were also studied. In these experiments, the concentration of NO released averaged 274 ± 18 ($n = 6$) and 219 ± 10 nM ($n = 6$), respectively. DEANO (*Figure 1C*) and the NO solution (*Figure 1D*) reduced the peak $I_{Kv4.3}$ by 35.5 ± 8.1 and 28.0 ± 5.8%, respectively. These values were not different from those obtained with the concentration of SNAP that released the same amount of NO ($P > 0.05$), indicating that, in all cases, the inhibition of $I_{Kv4.3}$ was exclusively due to NO. Moreover, neither DEANO nor the NO solution modified the time course of current decay (*Table 2*).

The Hill equation was used to fit the concentration dependence of peak current inhibition at +50 mV, yielding an IC_{50} of 391.8 ± 49.6 μM for SNAP ($n_H = 1.3 \pm 0.2$) (*Figure 1E*). When the inhibition was plotted as a function of the

released NO by SNAP (*Figure 1F*), the IC_{50} was 375.0 ± 47.8 nM ($n_H = 1.2 \pm 0.2$).

Figure 2A shows $I_{Kv4.3}$ traces obtained by applying 250 ms pulses from −80 mV to potentials between −90 and +50 mV (conditioning pulse) followed by a test pulse to +50 mV in the absence and presence of 200 μM SNAP. Current–voltage relationships (*Figure 2B*) show that SNAP significantly decreased peak $I_{Kv4.3}$ at potentials positive to −20 mV ($P < 0.05$). This reduction appeared in the range of potentials coinciding with that of channel activation (inhibition at −10 mV: 30.2 ± 5.5%), remaining unchanged at more positive potentials ($P > 0.05$). Inactivation curves (*Figure 2C*) were constructed by plotting the peak current amplitude elicited by the test pulse as a function of the conditioning pulse and by fitting a Boltzmann function to the data. SNAP decreased $I_{Kv4.3}$ between −90 and −30 mV and shifted V_h towards negative potentials without modifying the slope of the curve (*Table 2*). These voltage-dependent effects were also corroborated when DEANO and the NO solution were perfused (*Table 2*). Relative current was plotted as a function of the conditioning pulse, demonstrating that the inhibition remained unchanged at potentials between −90 mV (30.1 ± 4.5%) and −60 mV (34.0 ± 5.0%, $P > 0.05$) and, thereafter, it progressively increased at more positive potentials reaching a 62.3 ± 4.8% at −30 mV ($P < 0.05$ vs. inhibition at −90 mV).

3.2 Signalling pathways involved in the inhibition of $I_{Kv4.3}$

The guanylate cyclase (GC)/cGMP/PKG pathway is the most common mechanism implicated in NO effects.[2] To test the involvement of this pathway, the effects of SNAP in the presence of the GC inhibitor ^{1}H-[1,2,4]oxadiazolo[4,3-a] quinoxalin-1-one (ODQ) were studied. *Figure 3A* shows that 50 μM ODQ decreased the peak $I_{Kv4.3}$ at +50 mV by 27.0 ± 6.7%. The addition of SNAP (200 μM) further decreased the current by 29.2 ± 7.2% ($n = 5$), which was the same inhibition as that produced by SNAP alone ($P > 0.05$, *Figure 3C*). In the same way, after the perfusion with 500 μM 8-bromo-cGMP, a potent cell-permeable PKG activator, SNAP produced a 26.7 ± 4.9% inhibition of the current ($n = 4$, $P < 0.05$). These results suggested that the GC/cGMP/PKG pathway was not involved. To confirm that these results were not due to the expression system, we studied the effects of SNAP on Kv4.3-carried I_{to1} recorded in mouse ventricular myocytes by applying 250 ms pulses from −80 to +50 mV in the presence of 50 μM 4-aminopyridine (4-AP), which at this concentration, selectively inhibits I_{Kur}.[6] Under these conditions, 200 μM SNAP decreased I_{to1} by 27.3 ± 3.5% (not shown), and when SNAP was superfused in the presence of ODQ (inset in *Figure 3A*), the inhibition (30.9 ± 4.4%, $n = 5$) was not different from that produced by SNAP alone ($P > 0.05$). These data confirmed that the GC/cGMP/PKG pathway was not involved in the effects of NO on $I_{Kv4.3}$.

S-Nitrosylation, which is highly dependent on the cellular redox state, modifies the function of many proteins, including several receptors (ryanodine and neuronal NMDA)[17] and channels (hKv1.5).[11] Therefore, the effects of SNAP in the presence of the thiol-specific reducing agent, dithiothreitol (DTT), were studied. DTT reduced $I_{Kv4.3}$ by 35.4 ± 6.4% and the addition of SNAP further decreased the current by 25.8 ± 6.1% (*Figure 3C*, $n = 5$, $P > 0.05$), an inhibition similar to that produced in the absence of DTT. Therefore, S-nitrosylation was not involved in the NO effects on $I_{Kv4.3}$. However, the analysis of the amino acid sequence of Kv4.3 protein revealed at least two Cys (C131 and C132) located in an acid–base micro-environment, which can act as a catalyst for nitrosylation–denitrosylation of thiol residues.[17] A biotin switch assay followed by a western blot confirmed the presence of S-nitrosylated Cys residues on the Kv4.3 protein in donor-treated and untreated cells (*Figure 3B*). These results suggest that Kv4.3 channels belong to the 'nitrosylome', the pool of proteins that are S-nitrosylated in cells.[17]

The involvement of either the PKC or the Ca^{2+}/calmodulin-dependent protein kinase II (CaMKII) activation in the SNAP-induced inhibition was also discarded by performing experiments in the presence of the PKC inhibitor staurosporine (1 μM) or KN-93 (10 μM), a specific CaMKII inhibitor, respectively (*Figure 3C*).

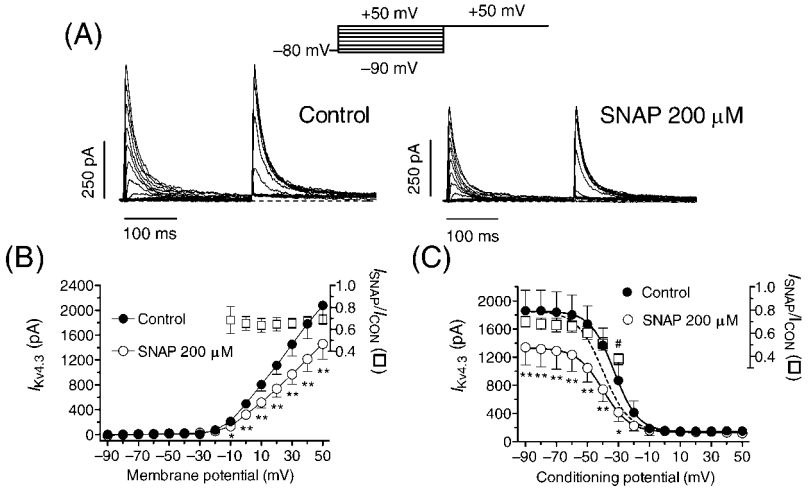

Figure 2 (*A*) $I_{Kv4.3}$ recorded in the absence and presence of *S*-nitroso-*N*-acetylpenicillamine (SNAP). (*B*) Mean $I_{Kv4.3}$ current–voltage relationships in the absence and presence of *S*-nitroso-*N*-acetylpenicillamine. (*C*) Inactivation curves of Kv4.3 channels in the absence and presence of *S*-nitroso-*N*-acetylpenicillamine. A Boltzmann equation was fitted to the data (continuous lines). The dashed line represents the curve in the presence of drug, normalized to the control amplitude. In (*B*) and (*C*), squares represent the relative current as a function of the membrane potential. Each point represents the mean ± SEM of five or more experiments. *$P < 0.05$ vs. control. **$P < 0.01$ vs. control. #$P < 0.05$ vs. inhibition at −90 mV.

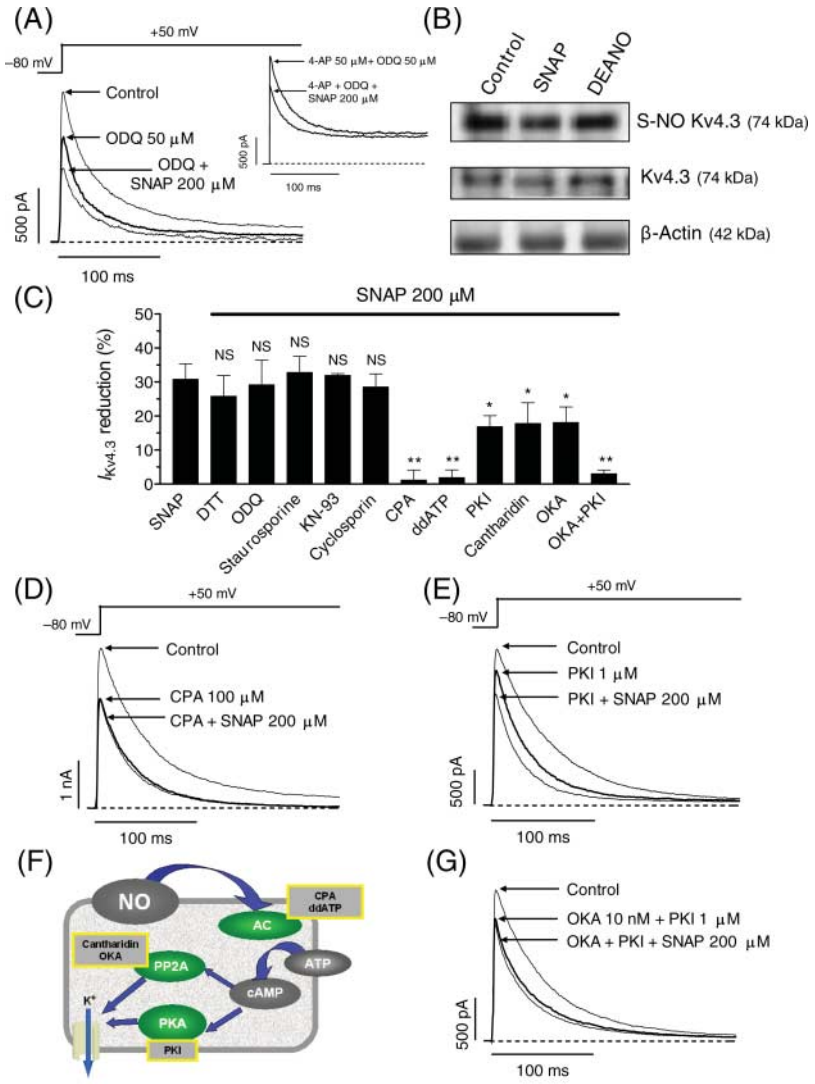

Figure 3 (*A*) $I_{Kv4.3}$ recorded in a Chinese hamster ovary cell in the absence and presence of ODQ alone and plus *S*-nitroso-*N*-acetylpenicillamine (SNAP). The inset shows I_{to1} traces recorded in a mouse ventricular myocyte in the presence of 4-AP + ODQ alone and plus *S*-nitroso-*N*-acetylpenicillamine. (*B*) Western blots showing S-nitrosylated Kv4.3, Kv4.3, and β-actin expression, in control conditions or after treatment with 200 μM *S*-nitroso-*N*-acetylpenicillamine and 3 μM 2-(*N*, *N*-diethylamine)-diazenolate-2-oxide (DEANO). (*C*) Percentage of inhibition produced either by *S*-nitroso-*N*-acetylpenicillamine alone or by *S*-nitroso-*N*-acetylpenicillamine in the presence of different inhibitors of enzymatic pathways. $I_{Kv4.3}$ recorded in control conditions and in the presence of (*D*) CPA or (*E*) PKI alone and plus *S*-nitroso-*N*-acetylpenicillamine. (*F*) Signalling pathway responsible for the nitric oxide effects. (*G*) $I_{Kv4.3}$ recorded in control conditions and in the presence of okadaic acid (OKA) + PKI without or with *S*-nitroso-*N*-acetylpenicillamine. $^{*}P < 0.05$ and $^{**}P < 0.01$ vs. *S*-nitroso-*N*-acetylpenicillamine alone.

To study whether the adenylate cyclase (AC)/cAMP/PKA pathway was involved in the inhibition of $I_{Kv4.3}$, we analysed the effects of SNAP in the presence of a membrane permeable (9-cyclopentyladenine, CPA, 100 μM) or an impermeable (2,5-dideoxy-ATP, ddATP, 200 nM) AC inhibitor, the latter being added to the internal solution. CPA (*Figure 3D*) and ddATP decreased $I_{Kv4.3}$ by 27.2 ± 4.8 ($n = 4$) and 20.4 ± 4.3% ($n = 4$), respectively, and the addition of 200 μM SNAP produced no effect on $I_{Kv4.3}$ (1.2 ± 2.5 and 1.9 ± 2.3%, respectively, *Figure 3C*). These results demonstrated that the SNAP-induced effects were mediated by the activation of the AC. In fact, after perfusion with 8-bromo-cAMP (500 μM), a cell-permeable cAMP analogue that inhibited $I_{Kv4.3}$ by 30.3 ± 2.3% ($n = 4$), SNAP did not further modify the $I_{Kv4.3}$ amplitude (2.8 ± 0.7%). However, in the presence of 1 μM PKI (a PKA inhibitor), SNAP decreased $I_{Kv4.3}$ by 16.9 ± 3.2% (*Figure 3E*), an inhibition significantly smaller than that produced by SNAP alone (*Figure 3C*, $n = 6$, $P < 0.05$). So, the effects of NO on Kv4.3 channels were only partially mediated via AC/cAMP/PKA.

It has been described that a cAMP-dependent methylation can increase the catalytic activity of serine/threonine phosphatase type 2A (PP2A),[18] and that the activation of PP2A inhibits I_{to1}.[13] Therefore, we also studied the effects of SNAP in the presence of okadaic acid (OKA), a PP2A inhibitor. OKA (10 nM) inhibited $I_{Kv4.3}$ by 15.4 ± 4.8%, and the addition of SNAP further decreased the current by 18.1 ± 4.6%, an inhibition significantly lower than that produced by SNAP alone (*Figure 3C*, $n = 5$, $P < 0.05$). Similar results were obtained when cantharidin was used as a PP2A inhibitor (17.8 ± 6.1%, $n = 6$, *Figure 3C*). Finally, to discard the putative implication of the serine/threonine phosphatase type 2B (calcineurin), which is known to be modulated by NO,[19] a group of experiments were performed in the presence of

cyclosporin (10 μM), which inhibits calcineurin. SNAP inhibited $I_{Kv4.3}$ in a similar way, both in the presence and absence of cyclosporin, which inhibited the current by $8.8 \pm 1.9\%$ ($n = 4$) (*Figure 3C*), discarding the implication of calcineurin on the NO inhibitory effects.

All these results demonstrated that the effects produced by SNAP were mediated by the activation of AC, which simultaneously activates the PKA and the PP2A (*Figure 3F*). This was further demonstrated because the simultaneous presence of PKI and OKA completely prevented the SNAP-induced inhibition (*Figures 3C* and *G*).

3.3 Effects of nitric oxide on I_{to1} on human atrial myocytes

We next studied the effects of SNAP on I_{to1} recorded in dissociated human LAA myocytes. A 25 ms prepulse to −30 mV was applied to inactivate I_{Na}, followed by a 250 ms pulse to +50 mV, eliciting an outward K^+ current which is composed of at least two currents: I_{to1} and I_{Kur}. In the presence of 50 μM 4-AP (to block I_{Kur}), SNAP 200 μM decreased I_{to1} amplitude by $24.9 \pm 1.2\%$ without modifying the time course of current decay ($\tau_{CON} = 39.9 \pm 2.9$ ms vs. $\tau_{SNAP} = 44.5 \pm 5.8$ ms, $P > 0.05$, $n = 5$) (*Figures 4A* and *F*).

Figures 4B, *C*, and *F* show that the inhibition of AC, with 100 μM CPA or 200 nM ddATP, also completely abolished the effects of SNAP on human I_{to1}. To test whether PKA activation was responsible for part of the effects, we analysed the effects of SNAP in the presence of 1 μM PKI (*Figure 4D*). Under these conditions, SNAP decreased the current by $11.5 \pm 2.9\%$ ($n = 4$), contrasting with the $24.9 \pm 1.2\%$ produced by SNAP alone ($P < 0.05$) (*Figure 4F*). Moreover, superfusion of OKA partially prevented the inhibition produced by SNAP ($13.2 \pm 4.9\%$, $n = 4$, *Figure 4F*), demonstrating that the activation of PP2A was also implicated (*Figure 4E*).

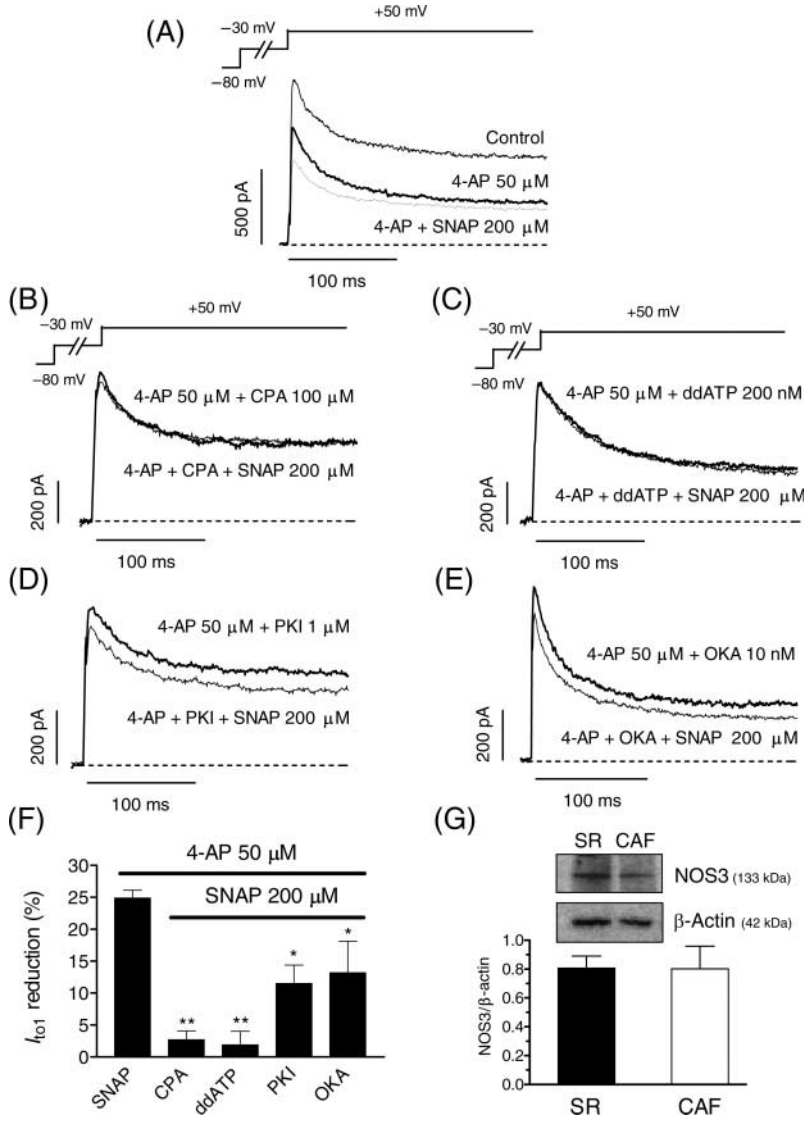

Figure 4 Effects of *S*-nitroso-*N*-acetylpenicillamine (SNAP) on I_{to1} recorded in human atrial myocytes in the presence of 4-AP (*A*), 4-AP + CPA (*B*), 4-AP + ddATP (*C*), 4-AP + PKI (*D*), or 4-AP + okadaic acid (OKA) (*E*). (*F*) Percentage of human I_{to1} inhibition produced by *S*-nitroso-*N*-acetylpenicillamine alone or in the presence of the different inhibitors of enzymatic pathways. (*G*) Nitric oxide synthase 3 and β-actin expression in left atrial appendages from sinus rhythm (SR) and chronic atrial fibrillation (CAF) patients and densitometric measurement of nitric oxide synthase 3 expression in left atrial appendages from sinus rhythm ($n = 5$) and chronic atrial fibrillation ($n = 7$) patients. *$P < 0.05$ and **$P < 0.01$ vs. *S*-nitroso-*N*-acetylpenicillamine alone.

3.4 Determination of the expression of nitric oxide synthase 3 in human atria

We also tested whether CAF could modify NOS3 expression. *Figure 4G* shows representative NOS3 western blots from LAA obtained from CAF and SR patients. The densitometric analysis revealed that the expression was not statistically different between the two groups ($P > 0.05$, $n = 11$).

3.5 I_{to1} and action potential characteristics in nitric oxide synthase 3-deficient mice

To elucidate whether the decrease in myocardial NO concentrations affected the I_{to1}, we compared the I_{to1} recorded in isolated ventricular myocytes from CD57 WT and NOS3$^{-/-}$ mice. *Figure 5A* shows families of currents recorded in the presence of 4-AP. The I_{to1} density–voltage relationships demonstrated that there were no differences in current density (I_{to1} amplitude/C_m) between the two groups (*Figure 5B*). Similarly, inactivation time course ($\tau_{WT} = 39.4 \pm 5.2$ ms and $\tau_{NOS3-/-} = 41.1 \pm 3.6$ ms) and the voltage dependence of I_{to1} inactivation ($V_{hWT} = -33.8 \pm 2.4$ and $V_{hNOS3-/-} = -38.9 \pm 2.2$ mV, *Figure 5C*) were not different ($n = 6$ in each group, $P > 0.05$).

WT and NOS3$^{-/-}$ multicellular atrial preparations were used for recording AP (*Figure 5D* and E). There was no difference between WT and NOS3$^{-/-}$ atrial preparations in the AP duration measured at 20 (APD_{20}), 50 (APD_{50}), and 90% (APD_{90}) of repolarization (*Figure 5F*). In contrast, AP amplitude (APA) was significantly lower in NOS3$^{-/-}$ (104.6 ± 3.9 mV, $n = 6$) than in WT preparations (119.2 ± 3.1 mV, $n = 6$, $P < 0.05$), even when no differences in the resting membrane potential (RMP) were found (RMP NOS3$^{-/-}$ = -83.2 ± 3.6 vs. RMP WT = -86.7 ± 3.1 mV, $n = 6$, $P > 0.05$). Finally, the effects of 200 μM SNAP on the AP characteristics were tested (*Figure 5D* and E). Both groups of atrial preparations responded identically to the increase in NO concentration. SNAP significantly decreased the APA by 6.0 ± 1.6 mV ($P < 0.05$) and hyperpolarized the RMP by 3.5 ± 1.2 mV

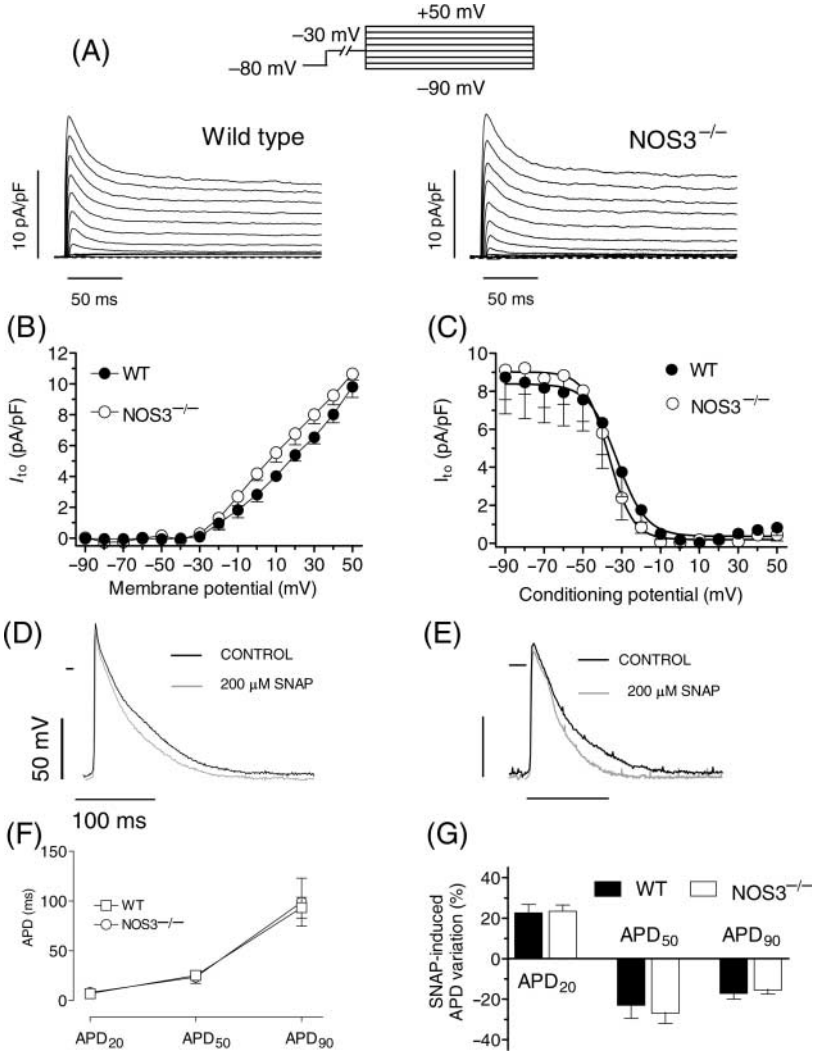

Figure 5 (*A*) Representative I_{to1} traces recorded in wild-type (WT) (left) and nitric oxide synthase 3-deficient (NOS3$^{-/-}$) (right) mouse ventricular myocytes in the presence of 4-AP. (*B*) Mean I_{to1} density-voltage relationships in wild-type and nitric oxide synthase 3-deficient mouse myocytes. (*C*) Inactivation curves of I_{to1} in wild-type and nitric oxide synthase 3-deficient mouse myocytes. A Boltzmann equation was fitted to the data (continuous lines). (*D* and *E*) Action potentials recorded in left atrial multicellular preparations from wild-type (*D*) and nitric oxide synthase 3-deficient (*E*) mice in the absence and presence of *S*-nitroso-*N*-acetylpenicillamine (SNAP). (*F*) APD measured at 20, 50, and 90% of repolarization in left atria from wild-type and nitric oxide synthase 3-deficient mice. (*G*) Percentage of change in the APD produced by *S*-nitroso-*N*-acetylpenicillamine in wild-type and nitric oxide synthase 3-deficient mice. Each point and bar represents the mean ± SEM of six or more experiments.

($P < 0.05$). Repolarization was also affected by SNAP, so that APD_{20} was significantly prolonged by ~25% (from 6.3 ± 0.8 to 7.8 ± 1.0 ms in WT and from 6.0 ± 0.7 to 7.5 ± 0.9 ms in $NOS3^{-/-}$ mice, respectively, $P < 0.05$), whereas APD_{50} and APD_{90} were significantly shortened (*Figure 5G*).

3.6 Effects of nitric oxide on a mathematical model of chronic atrial fibrillation-modified action potentials

We ran a previously described model of a human atrial AP in SR and in CAF-simulated conditions.[16] To simulate the electrophysiological remodelling in CAF, reductions of 70% in I_{CaL}, and of 50% in I_{to1} and I_{Kur}, were introduced as described (*Figure 6C* and *D*). These modifications produced indirect changes of other currents (i.e. a reduction in I_{Kr}, I_{Ks}, and I_{NaCa}) (compare panels *E* and *F*), resulting in the characteristic triangular shape and shortening of APs in CAF.[16] *Figure 6* shows the AP in SR (panel *A*) and CAF conditions (panel *B*) in the absence of (continuous line), and after increasing, the NO concentration to 200 nM (dashed line). The latter was run by incorporating the effects produced by NO ~200 nM in the currents shown in *Figures 6C–F*. I_{to1} was decreased by 30.8% as described in this paper. For the other currents, we introduced the data previously reported in the literature regarding the effects of NO. Indeed, 200 μM SNAP decreased I_{CaL}, I_{Kur}, and I_{Kr} by 40, 31, and 45%, respectively.[8,9,11] Moreover, 200 nM NO reduced I_{Na} by 5%,[20] whereas 200 μM sodium nitroprusside increased I_{Ks} by 20%.[10] In non-AF conditions, NO-combined blockade of I_{to1}, I_{Kur}, I_{CaL}, and I_{Kr} produced a dynamic change in I_{Ks} which overcame the NO-induced increase in this latter current. The global result was a slight prolongation of the APD_{20} and a shortening of the APD_{50} by 12.5%. In CAF conditions, NO blockade of I_{Kur} and I_{to1} would lead to a prolongation of the APD_{20} and APD_{50} of 25 and 27%, respectively. This result can be understood considering that the decrease in I_{CaL} produced by CAF reduces its role in shaping the AP. Moreover, the small increase in the plateau height and duration produced dynamic modifications in the I_{Kr} and I_{Ks} amplitudes which combined with the NO-induced I_{Kr} block and I_{Ks} increase led to a shortening in the APD_{90}.

4. Discussion

The present results demonstrated that (i) NO and NO donors (SNAP and DEANO) inhibited $I_{Kv4.3}$ and human atrial I_{to1}.

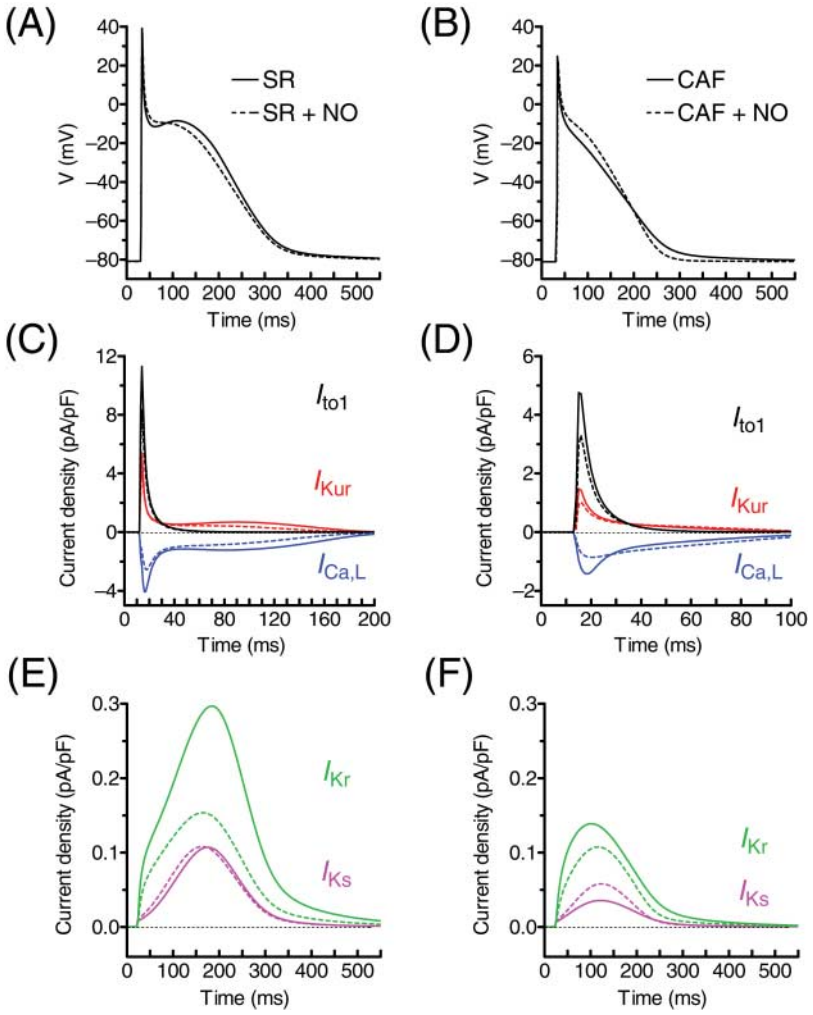

Figure 6 Mathematical modelling of human atrial action potentials in normal conditions (sinus rhythm, *A*) and in patients with chronic atrial fibrillation (70% reduction in I_{CaL} and 50% in I_{to1} and I_{Kur}, *B*) in the absence and after establishing the nitric oxide levels at 200 nM. The model in the presence of nitric oxide was run by incorporating the effects produced by nitric oxide on the currents shown in (*C*)–(*F*). The currents are the results of both the nitric oxide effects and the dynamic modifications that they produced on the action potential morphology.

(ii) NO inhibition was mediated by the activation of AC and the subsequent activation of PKA and PP2A. (iii) LAA from CAF patients presented the same NOS3 expression level as in SR patients. (iv) There was no difference in the I_{to1} characteristics measured in ventricular myocytes from WT and NOS3$^{-/-}$ mice. (v) The increase in NO levels to 200 nM prolonged the plateau phase of the mouse atria, and lengthened the APD_{20} and APD_{50} of the human atrial CAF-modified AP as determined using a mathematical model.

4.1 Signalling pathways involved in the effects of nitric oxide on $I_{Kv4.3}$ and I_{to1}

NO produced a concentration-dependent inhibition of $I_{Kv4.3}$ which was reproduced in human atrial I_{to1}. The observation that the NO solution and two chemically dissimilar NO donors, whose only common denominator is their ability to release NO, inhibit $I_{Kv4.3}$ in a qualitatively and quantitatively similar manner suggests that this modulation is mediated by NO and not by the consequence of other NO-independent mechanisms.

The inhibition of I_{to1} by NO was independent of the main pathways involved in NO effects in other substrates (GC/cGMP/PKG pathway, PKC activation, or redox-dependent post-translational modifications).[2,17] The mechanism responsible for NO inhibition of $I_{Kv4.3}$ and human I_{to1} was the activation of AC (which can be activated by NO through a mechanism that involves G proteins)[21] and the subsequent activation of AC/cAMP/PKA pathway and PP2A. Other studies demonstrated that increased cAMP generation may be able to stimulate dephosphorylation of proteins. Indeed, an increase in cAMP levels can activate the PP2A by increasing the rates of PP2A methylation.[18] Previous reports demonstrated that the activation of either the AC/cAMP/PKA pathway or the PP2A can inhibit human and rat I_{to1}[6,13,22] and that the AC/cAMP/PKA pathway is responsible for the NO inhibition of cardiac I_{Na}.[20]

The results suggest that the PKA phosphorylation and PP2A dephosphorylation take place in the Kv4.3 proteins and not in one of the ancillary β-subunits that form the native channel complex. Though it may be somewhat surprising that Kv4.3 is regulated by its simultaneous phosphorylation and dephosphorylation, this is not the first example of such a mechanism of regulation. Indeed, activation of NOS3 promoted by heat shock protein 90 involves its phosphorylation and dephosphorylation in two different residues.[23] Similarly, PP2A dephosphorylation of the Kv4.3 protein probably takes place in a different residue than the PKA phosphorylation site, like the PKC or the PKG phosphorylation sites.[22]

4.2 Putative role of nitric oxide in electrical changes in chronic atrial fibrillation

Our results suggest that CAF does not modify NOS3 expression in human LAA. This is in agreement with the findings by Cai *et al.*,[3] who demonstrated in a porcine model of AF that NOS3 expression in the LAA did not differ from that in control animals despite the reduction in NO formation at this site. However, in other parts of the atria, the authors did find a significant decrease in NOS3 expression. Moreover, there is another report using a canine model of AF demonstrating an increase in NOS3 expression.[24] Thus, caution should be exerted in extrapolating the present finding to the whole atria. Finally, it has to be considered that the characteristics and/or the pharmacological treatment of the patients could also have determined the NOS3 expression level.

What is clearly established, both in patients and in animal models, is that NO bioavailability decreases in AF because of the increased atrial oxidative stress which scavenges NO to form the potent oxidant peroxynitrite and 'uncouples' NOS activity.[4,5] This increase in the oxidative stress and decrease in NO concentrations may play an important role in the atrial oxidative injury and electrophysiological remodelling observed in CAF patients. The key role of NO in AF has also been suggested by the presence of a polymorphism in the NOS3 as a predisposing factor to AF.[25]

The present results demonstrated that prolonged decrease in NO concentrations does not modify the I_{to1} density in NOS3$^{-/-}$ mouse myocytes. This result is similar to that previously reported for I_{CaL} density.[26] These authors used the same knockout strain as that used in the present experiments, in which it has been demonstrated that NOS3 suppression does not produce an upregulation of the neuronal and inducible isoforms of the NOS, and that the nitrite/nitrate levels were significantly decreased compared with WT.[26,27] Recent reports stressed the important role of Kv4.2 alpha subunits (together with Kv4.3) in generating the I_{to1} channels in the mouse heart.[28] We also tested the effects of SNAP on $I_{Kv4.2}$ resulting in an inhibition of the current ($30.4 \pm 3.8\%$, $n = 5$, $P < 0.05$, not shown) not different from that produced on $I_{Kv4.3}$. Thus, it seems difficult to attribute the lack of effects of chronic NO deficiency on I_{to1} to the heteromeric composition of the channel. Therefore, it seems reasonable to assume that the decrease of NO itself cannot account for the decrease in Kv4.3 expression observed in CAF patients.

Here we demonstrate that NO, at physiological concentrations (200–900 nM),[29] inhibited human I_{to1}. In SR patients, AP is shaped by the presence of these physiological concentrations of NO, whereas in CAF patients, in which NO bioavailability is markedly decreased, the absence of NO could modify the AP characteristics. Thus, we analyse the effects of NO on CAF-modified AP by running a mathematical model previously validated for similar purposes,[16] by incorporating all the described effects of NO in human atrial ionic currents. However, a limitation of this approach is that the effects of NO on each individual current were obtained under different experimental conditions (native currents and transfected cloned channels) and in healthy cells dissociated from hearts of different species. The model predicted that 200 nM NO would prolong the plateau phase of CAF-remodelled atrial AP. Furthermore, the plateau phase prolongation was confirmed when the effects of SNAP were analysed in multicellular preparations from WT and NOS3$^{-/-}$ mice. In this case, SNAP prolonged the APD_{20} by 25%, whereas it shortened both the APD_{50} and APD_{90}. The discrepancy observed in the effects produced on the APD_{50} could be attributed to unknown effects produced by SNAP on outward K^+ currents exclusively present in the mouse myocardium.

In human atria, the inhibition of I_{Kur} and I_{to1} would increase the height and duration of the plateau,[15] a prolongation that was critical for the termination of the periodic activity of sustained, high frequency, functional re-entrant sources (rotors), which could be responsible for

AF.[30] In fact, rotor termination was related to a prolongation of the APD at the plateau, rather than at the terminal phase of repolarization. In this respect, it has to be stressed that the combined inhibition of I_{to1} and I_{Kur}[11] produced by NO results in a prolongation of the plateau duration in human CAF-remodelled AP, which reached 83% at 30% of repolarization.

Overall, the results presented here suggest that the increase in atrial NO bioavailability could prolong the duration of the plateau phase of CAF-remodelled AP by inhibiting the I_{to1} as a result of the activation of AC, which in turn activates PKA and PP2A. Therefore, the presence of physiological NO concentrations in the human atria could contribute to the prevention and/or cessation of the AF by the modulation of I_{to1} and I_{Kur}. Thus, it is tempting to speculate that drugs that increase NO availability may exert a beneficial effect in patients with CAF. In fact, interventions that prevent activation of NADPH oxidases by vasoactive hormones or pro-inflammatory cytokines (i.e. angiotensin-converting enzyme-inhibitors, angiotensin II receptor blockers, or statins) are highly effective in preventing the occurrence of AF in patients with hypertension, heart failure or after heart surgery.[1]

Funding

Supported by Ministerio de Educación y Ciencia (SAF2005-04609), Ministerio de Sanidad y Consumo, Instituto de Salud Carlos III (Red HERACLES RD06/0009), Sociedad Española de Cardiología, and Fundación LILLY. Ricardo Gómez is a fellow of Comunidad Autónoma de Madrid.

Acknowledgements

We thank Guadalupe Pablo for her excellent technical assistance and Drs T. Pérez-García and J.R. López-López (School of Medicine, Valladolid University, Spain) for the generous gift of the Kv4.2 cDNA.

Conflict of interest: none declared.

References

1. Casaclang-Verzosa G, Gersh BJ, Tsang TS. Structural and functional remodeling of the left atrium: clinical and therapeutic implications for atrial fibrillation. *J Am Coll Cardiol* 2008;**51**:1–11.
2. Massion PB, Feron O, Dessy C, Balligand JL. Nitric oxide and cardiac function: ten years after, and continuing. *Circ Res* 2003;**93**:388–389.
3. Cai H, Li Z, Goette A, Mera F, Honeycutt C, Feterik K *et al*. Downregulation of endocardial nitric oxide synthase expression and nitric oxide production in atrial fibrillation: potential mechanisms for atrial thrombosis and stroke. *Circulation* 2002;**106**:2854–2858.
4. Kim YM, Guzik TJ, Zhang YH, Zhang MH, Kattach H, Ratnatunga C *et al*. A myocardial Nox2 containing NAD(P)H oxidase contributes to oxidative stress in human atrial fibrillation. *Circ Res* 2005;**97**:629–636.
5. Carnes CA, Chung MK, Nakayama T, Nakayama H, Baliga RS, Piao S *et al*. Ascorbate attenuates atrial pacing-induced peroxynitrite formation and electrical remodeling and decreases the incidence of postoperative atrial fibrillation. *Circ Res* 2001;**89**:e32–e38.
6. Tamargo J, Caballero R, Gómez R, Valenzuela C, Delpón E. Pharmacology of cardiac potassium channels. *Cardiovasc Res* 2004;**62**:9–33.
7. Campbell DL, Stamler JS, Strauss HC. Redox modulation of L-type calcium channels in ferret ventricular myocytes. Dual mechanism regulation by nitric oxide and *S*-nitrosothiols. *J Gen Physiol* 1996;**108**:277–293.
8. Hu H, Chiamvimonvat N, Yamagishi T, Marbán E. Direct inhibition of expressed cardiac L-type Ca^{2+} channels by *S*-nitrosothiol nitric oxide donors. *Circ Res* 1997;**81**:742–752.
9. Taglialatela M, Pannaccione A, Iossa S, Castaldo P, Annunziato L. Modulation of the K^+ channels encoded by the human ether-a-gogo-related gene-1 (hERG1) by nitric oxide. *Mol Pharmacol* 1999;**56**:1298–1308.
10. Bai CX, Takahashi K, Masumiya H, Sawanobori T, Furukawa T. Nitric oxide-dependent modulation of the delayed rectifier K^+ current and the L-type Ca^{2+} current by ginsenoside Re, an ingredient of *Panax ginseng*, in guinea-pig cardiomyocytes. *Br J Pharmacol* 2004;**142**:567–575.
11. Núñez L, Vaquero M, Gómez R, Caballero R, Mateos-Cáceres P, Macaya C *et al*. Nitric oxide blocks hKv1.5 channels by S-nitrosylation and by a cyclic GMP-dependent mechanism. *Cardiovasc Res* 2006;**72**:80–89.
12. Radicke S, Cotella D, Graf EM, Banse U, Jost N, Varro A *et al*. Functional modulation of the transient outward current I_{to} by KCNE beta-subunits and regional distribution in human non-failing and failing hearts. *Cardiovasc Res* 2006;**71**:695–703.
13. Caballero R, Gómez R, Moreno I, Núñez L, González T, Arias C *et al*. Interaction of angiotensin II with the angiotensin type 2 receptor inhibits the cardiac transient outward potassium current. *Cardiovasc Res* 2004;**62**:86–95.
14. Vaquero M, Caballero R, Gómez R, Núñez L, Tamargo J, Delpón E. Effects of atorvastatin and simvastatin on atrial plateau currents. *J Mol Cell Cardiol* 2007;**42**:931–945.
15. Wettwer E, Hála O, Christ T, Heubach JF, Dobrev D, Knaut M *et al*. Role of I_{Kur} in controlling action potential shape and contractility in the human atrium. Influence of chronic atrial fibrillation. *Circulation* 2004;**110**:2299–2306.
16. Courtemanche M, Ramírez RJ, Nattel S. Ionic targets for drug therapy and atrial fibrillation induced electrical remodeling: insights from a mathematical model. *Cardiovasc Res* 1999;**42**:477–489.
17. Martínez-Ruíz A, Lamas S. S-nitrosylation: a potential new paradigm in signal transduction. *Cardiovasc Res* 2004;**62**:43–52.
18. Floer M, Stock J. Carboxyl methylation of protein phosphatase 2A from Xenopus eggs is stimulated by cAMP and inhibited by okadaic acid. *Biochem Biophys Res Commun* 1994;**198**:372–379.
19. Hara MR, Snyder SH. Cell signaling and neuronal death. *Annu Rev Pharmacol Toxicol* 2007;**47**:117–141.
20. Ahmmed GU, Xu Y, Hong Dong P, Zhang Z, Eiserich J, Chiamvimonvat N. Nitric oxide modulates cardiac Na^+ channel via protein kinase A and protein kinase G. *Circ Res* 2001;**89**:1005–1013.
21. Lander HM, Sehajpal PK, Novogrodsky A. Nitric oxide signaling: a possible role for G proteins. *J Immunol* 1993;**151**:7182–7187.
22. Van der Heyden MA, Wijnhoven TJ, Opthof T. Molecular aspects of adrenergic modulation of the transient outward current. *Cardiovasc Res* 2006;**71**:430–442.
23. Kupatt C, Dessy C, Hinkel R, Raake P, Daneau G, Bouzin C *et al*. Heat shock protein 90 transfection reduces ischemia–reperfusion-induced myocardial dysfunction via reciprocal endothelial NO synthase serine 1177 phosphorylation and threonine 495 dephosphorylation. *Arterioscler Thromb Vasc Biol* 2004;**24**:1435–1441.
24. Shiroshita-Takeshita A, Brundel BJ, Lavoie J, Nattel S. Prednisone prevents atrial fibrillation promotion by atrial tachycardia remodeling in dogs. *Cardiovasc Res* 2006;**69**:865–875.
25. Bedi M, McNamara D, London B, Schwartzman D. Genetic susceptibility to atrial fibrillation in patients with congestive heart failure. *Heart Rhythm* 2006;**3**:808–812.
26. Gödecke A, Heinicke T, Kamkin A, Kiseleva I, Strasser RH, Decking UK *et al*. Inotropic response to beta-adrenergic receptor stimulation and anti-adrenergic effect of ACh in endothelial NO synthase-deficient mouse hearts. *J Physiol* 2001;**532**:195–204.
27. Gödecke A, Decking UK, Ding Z, Hirchenhain J, Bidmon HJ, Gödecke S *et al*. Coronary hemodynamics in endothelial NO synthase knockout mice. *Circ Res* 1998;**82**:186–194.
28. Niwa N, Wang W, Sha Q, Marionneau C, Nerbonne JM. Kv4.3 is not required for the generation of functional Ito,f channels in adult mouse ventricles. *J Mol Cell Cardiol* 2008;**44**:95–104.
29. Malinski T. Understanding nitric oxide physiology in the heart: a nanomedical approach. *Am J Cardiol* 2005;**96**:13i–24i.
30. Pandit SV, Berenfeld O, Anumonwo JM, Zaritski RM, Kneller J, Nattel S *et al*. Ionic determinants of functional reentry in a 2-D model of human atrial cells during simulated chronic atrial fibrillation. *Biophys J* 2005;**88**:3806–3821.